

A SILICON CARBIDE DIFFERENTIAL OUTPUT PRESSURE SENSOR BY CONCENTRICALLY MATCHED CAPACITANCE

Levent Beker¹, Ayden Maralani², Liwei Lin¹, and Albert P. Pisano²

¹Mechanical Engineering, University of California, Berkeley, CA, USA

²Mechanical and Aerospace Engineering, University of California, San Diego, CA, USA

ABSTRACT

This work describes a silicon-carbide (SiC) based, micromachined harsh-environment pressure sensor that utilizes concentrically matched differential capacitance output (DCO) to transfer relatively small capacitance changes through very long cables and reduce signal noises. By utilizing the concentrically matched capacitance (CMC) design, sensors with DCO can be fabricated by a newly developed SiC surface micromachining process. Experimentally, the sensor has measured pressure diaphragm output of 1.4 pF and 1.2 pF under 1.4 MPa at temperatures of 20°C and 180°C, respectively, while the reference ring diaphragm stays as a constant at 0.14 pF. As such, this sensor could be mounted along long cables to transfer small capacitance changes without any active electronics for harsh-environment applications, such as geothermal wells, engines, and turbines.

INTRODUCTION

Geothermal energy is one of the few untapped energy resources derived from the earth's heat and becomes even more critical because it supplies renewable energy and emits little or no greenhouse gasses [1]. However, harnessing geothermal energy sources efficiently is not trivial and requires continuous monitoring of wellbore conditions (pressure and temperature) using sensors and electronics that can operate in high temperature and high pressure environments as depicted in Figure 1a. Because of high temperatures and high costs of replacement and maintenance, battery powered stand-alone systems are not practical. Therefore, these monitoring systems are mounted along several km's long cables inside the earth's surface. Usually, these sensors are deployed along kilometers of long cables inside pipes having 4"-10" diameters without blocking fluid flow through the pipe such that the sensors should have small sizes. In addition to the harsh environmental conditions, transferring data of pressure change signals through long cables brings additional challenges.

Recent efforts to develop sensors for monitoring wellbore conditions include fiber-optic and SiC based pressure sensors. Although these efforts utilize harsh environment sensors, they lack in transferring signals through long cables. Xiao *et al.* proposed a fiber-optic pressure sensor that can operate up to 58 MPa [2]. However, degradation of optical fibers is a common problem that prevents the implementation of optic-fiber based sensors within high temperature environments. Chen *et al.* presented a SiC capacitive pressure sensor with

characterizations under 5 MPa at temperature of 574°C [3]. However, a small change of capacitance (on the order of picoFarads) obtained during the tests won't be transferred through kilometer-long cables due to noise effects. On the other hand, the principle DCO sensing has been reported many years ago to eliminate the noise effects. Moe *et al.* proposed a pressure sensor with DCO and characterized the sensor up to 175°C [4]. However, this sensor requires a complex fabrication process including two wafer bonding steps. Recently, McNeil *et al.* filed a patent for a sensor that makes use of a lever-like system which has DCO operation [5]. However, this sensor also requires a complicated fabrication flow such that the lever structure has to be integrated to a thin diaphragm.

DESIGN

In this study, we present a SiC-based CMC sensor that can be fabricated in a similar way like the conventional capacitive pressure sensors as well as to be designed with the DCO so that it can be integrated into conventional circuit schemes to read small signals from long distances. Figure 1b depicts the quad-diode bridge circuit coupled with a DCO pressure sensor to eliminate common-mode noise stemming from km-long cables [6].

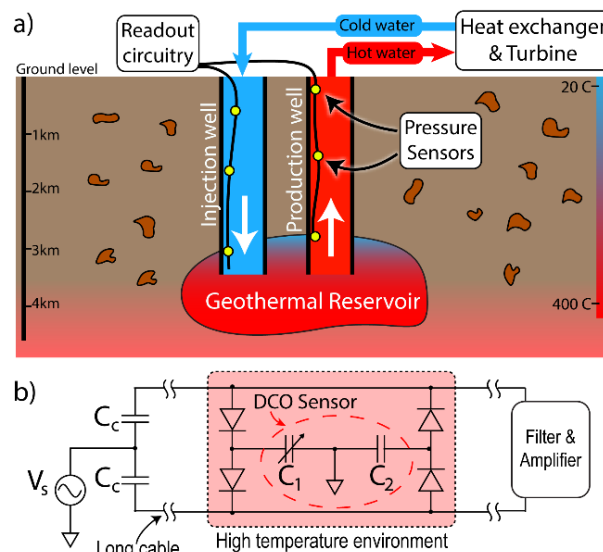


Figure 1: a) Geothermal energy generation process in a well and implementation of harsh-environment sensors along the long cables; b) the differential capacitance output (DCO) sensor coupled with a quad-diode bridge circuit to eliminate common-mode noise stemming from the long-cables.

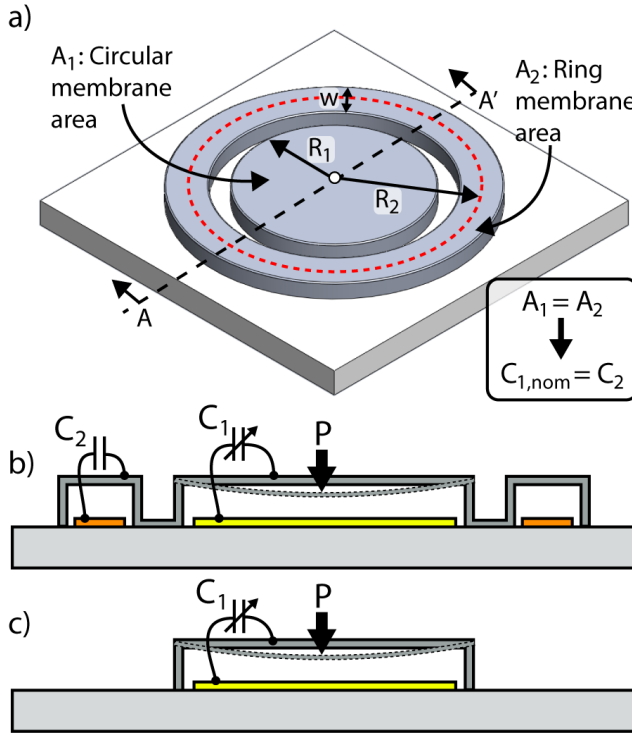


Figure 2: a) The design of the concentrically matched capacitance (CMC) pressure sensor; b) cross-sectional view of the proposed sensor along A-A'; c) cross-sectional view of a conventional capacitive pressure sensor which has only one capacitance output.

Figure 2a shows the proposed sensor which consists of a concentric circular and ring-shape membranes with the same foot-prints such that they have the same nominal capacitance, and its critical design parameters. Figures 2b and 2c show the cross-sectional views and device operation for the proposed CMC design and conventional sensors, respectively. When the external pressure is applied, the circular membrane deforms and the capacitance between the circular membrane and substrate, C_1 , increases. This operation is the same as the one used in the conventional pressure sensors. In addition to the circular membrane, the proposed design has the ring membrane which has a higher stiffness compared to the circular membrane. Therefore, the deflection of the ring membrane is negligible compared to the circular membrane such that the capacitance between the ring and the substrate, C_2 , stays the same and can serve as a reference capacitor.

Equations (1) and (2) can be used to calculate the maximum deflections under an applied pressure for the circular membrane (δ_c) and ring-shape membrane (δ_r), respectively [7], [8].

$$\delta_c = \frac{PR_1^4}{64D + 4\sigma_f t R_1^2} \quad (1)$$

$$\delta_r = \frac{PR_2^2}{D} [\varphi_1(R_2, w) + R_2 \varphi_2(R_2, w) + R_2^2 \varphi_3(R_2, w)] \quad (2)$$

where P is the external pressure; R_1 is the radius of the circular membrane; R_2 and w are the center radius and width of the ring membrane, respectively; D is the flexural stiffness; σ_f is film stress; t is membrane thickness; and φ_1 , φ_2 , and φ_3 are geometric functions dependent on R_2 and w . In addition to the Equations (1-2), Comsol finite-element (FE) modelling program is also used to determine the deflections of the structures. For simulation purposes, an external pressure of 1 MPa was applied to 2 μm -thick SiC circular and ring membranes having R_1 and R_2 of 100 μm and 136 μm , respectively. Figure 3 summarizes both the FE simulation and analytical results of the deflections at the centers of the circular and ring membranes, while Table 1 gives the SiC material properties used in the simulation. The simulation results match closely with the analytical results and for the pressure range between 100 kPa to 2 MPa as deflection ratio (δ_c / δ_r) changes from 340 to 130. This confirms that the deflection of the ring membrane is negligible as compared to that of the circular membrane under the same pressure.

Table 1: Material properties used in the simulation.

Young's Modulus	Poisson's ratio	Density
401 GPa	0.17	3210 kg/cm ³

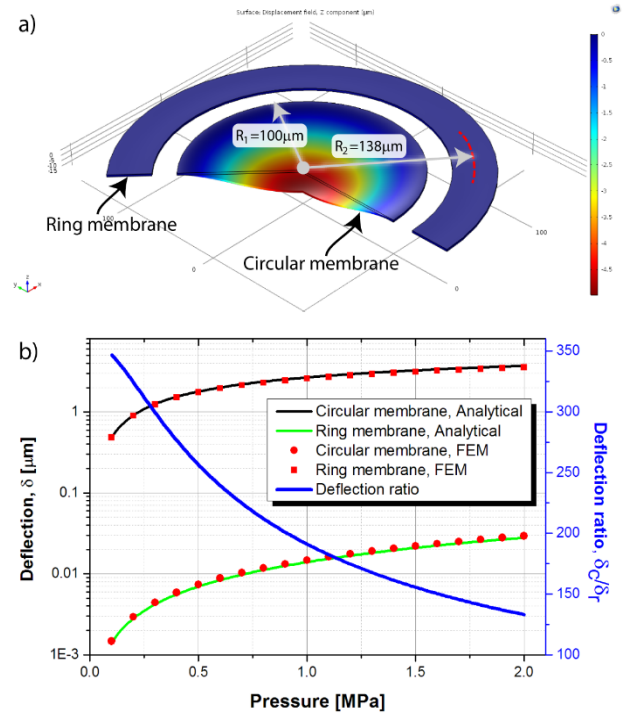


Figure 3: a) Finite-element simulation results showing the deflection contour of the proposed sensor having dimensions of $R_1=100\mu\text{m}$, $R_2=138\mu\text{m}$, and $w=36\mu\text{m}$ under the pressure of 1 MPa; b) comparison of the deflection of the circular and ring membranes by finite-element and analytical model under various magnitudes of external pressure for sensors with dimensions given in a.

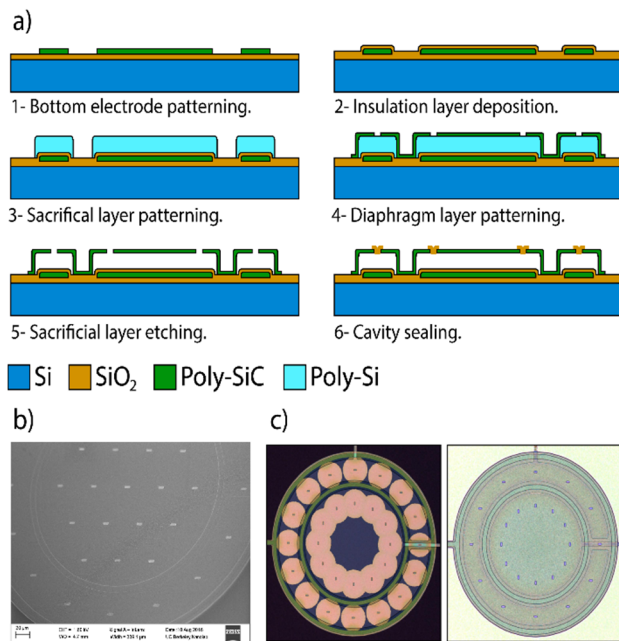


Figure 4: a) Fabrication process flow of the sensors; b) SEM image of a fabricated sensor; c) optical images during the XeF₂ vapor etching process (left) and after the removal of the poly-Si sacrificial layer.

FABRICATION

Figure 4a shows the fabrication flow of the proposed CMC pressure sensor. The fabrication process starts with the deposition of an oxide layer on top of a <100> Si wafer which serves as an insulation layer. Then, a 0.5 μ m-thick poly-SiC layer is deposited to serve as bottom electrodes via the low pressure chemical vapor deposition (LPCVD) process at 800 $^{\circ}$ C which is then followed by lithography and etching via reactive ion etching (RIE) of the poly-SiC layer using Mask #1. In order to prevent the short circuit between the diaphragm and the bottom electrode, an oxide layer is again deposited, patterned and etched using Mask #2. A sacrificial poly-Si was deposited using the plasma enhanced CVD process and patterned to define membrane boundaries and gap height using Mask #3. A second poly-SiC layer is deposited, patterned and etched using Mask #4 to define the membranes and openings is defined on the poly-SiC membranes by etching sacrificial poly-Si via XeF₂ vapor based etching process as shown in Figure 4c. In order to relieve the diaphragm stress, the wafer is annealed at 700 $^{\circ}$ C. Then, the openings are sealed by the deposition and patterning an oxide layer via an LPCVD process at 450 $^{\circ}$ C using Mask #4. The cavities are designed to have widths of 1-2 μ m, so that they seal before oxide builds up inside the diaphragm. In addition, the cavity sealing process is held at pressure of 40 Pa, which makes the sensors to be sensitive under 1 atm (~101 kPa). Finally, a metal layer was deposited and patterned for electrical contacts using Mask #5.

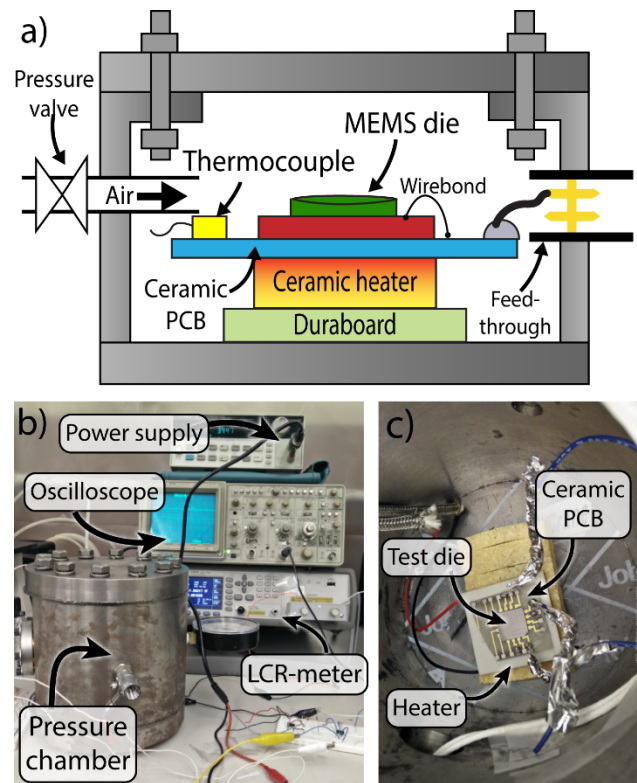


Figure 5: a) Schematic diagram of the temperature controlled pressure chamber built for characterization of the sensors; photo of b) the test setup, c) inside the pressure chamber.

RESULTS

Figure 5 shows the temperature controlled pressure chamber experimental setup that is used for the characterization of the sensors. The fabricated sensors were attached to a high-temperature stable aluminum nitride (AlN) printed circuit board (PCB) which was then mounted onto a ceramic heater for high temperature tests. Capacitance changes of the sensors were measured by using an LCR-meter while temperature of the sensors was measured by a thermocouple and controlled by the ceramic heater both of which are assembled to the AlN PCB. Due to the limitations of the test setup and safety regulations, pressure sensors were tested up to 1.4 MPa at 180 $^{\circ}$ C.

Figure 6 shows experimental results of the sensors. The tested sensors have thickness of 2 μ m, circular membrane radius of 80 μ m and ring's inner and outer radii of 90 μ m and 120 μ m, respectively. The test was held in the pressure range of 100 kPa to 1.4 MPa (with steps of 100 kPa) and at temperatures of 20 $^{\circ}$ C, 100 $^{\circ}$ C, and 180 $^{\circ}$ C. Five measurements were recorded for each pressure and temperature conditions. During the measurements, both non-contact and contact modes of the sensor is visible in the capacitance-pressure plot with contact-mode operation starting at around 0.5 MPa. Generally the contact-mode operation of circular diaphragms is considered to be in

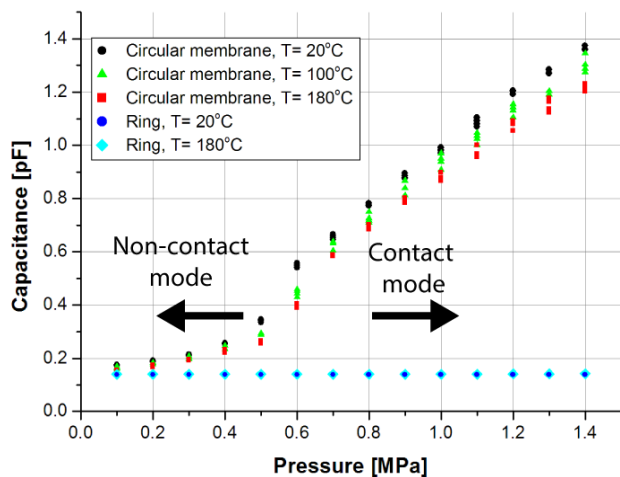


Figure 6: Experimental results showing the capacitance changes of the circular and ring membranes with respect to pressure under various temperatures of 20°C, 100°C and 180°C

1.5x-3x that of the touch pressure. Considering this region as the operation range for contact-mode operation, the sensor achieved a sensitivity of 1.03 fF/kPa at room temperature. As the temperature increases, results show the decrease in capacitance and sensitivity, and sensitivities of 0.98 fF/kPa and 0.92 fF/kPa at 100°C and 180°C, respectively. The decrease in both the capacitance and the sensitivity is believed to be the increased diaphragm stress at higher temperatures and stiffened diaphragm to cause smaller deformations.

Although, the increased temperature has resulted in reduction in capacitance and sensitivity for the circular membrane, the capacitance of the ring membrane was almost constant at tested temperatures; thus, successfully verify the DCO-operation of the sensor. The DCO-operation of the sensor was verified at temperatures of 20°C and 180°C and capacitance of 0.14 pF was obtained for both cases.

CONCLUSIONS

Concentric circular and ring membranes with matched capacitance have been designed, fabricated, and tested. Fabrication of the proposed sensors is very similar to that of the conventional sensors and can be fabricated using a single structural layer. The proposed design allows measurement of pressure and can provide DCO. Applications that need deployment of sensors in remote areas using long cables or in high temperature environments require sensors to have DCO in order to prevent noise effects. Therefore, the proposed sensor allows measurement of pressure for these applications, such as geothermal wells and automotive engines. Furthermore, because the proposed structure is similar to conventional sensors, it is possible to fabricate the proposed design using the same fabrication flow of the conventional sensors without any complex fabrication

steps as in the mentioned earlier efforts. In addition to the CMC design, SiC is used as the structural layer which can withstand high temperatures. The fabricated sensors were tested in pressure of up to 1.4 MPa at 180°C. Although, a reduction in the capacitance and sensitivity was observed for the circular membrane, there was almost no change in the capacitance of the ring membrane under various temperatures and pressures. It is believed that such kind of sensor will be useful for harsh environment applications. In future studies, we will be integrating the sensors to the quad-diode bridge to verify the operation of transferring small capacitance changes along long-cables and build a test setup which can withstand higher temperatures and pressures.

ACKNOWLEDGEMENTS

The authors would like to thank Dr. Kirti Mansukhani, Dr. Grzegorz Cieslewski, and Douglas Blankenship for their valuable discussions and Sandia National Laboratories and the Department of Energy for their support. The authors also would like to thank Dr. Duy Son Nguyen, Rich Hemphill and Marvell Nanolab staff for helpful discussions on the fabrication of the device. Levent Beker is supported by the Howard Hughes Medical Institute International Student Fellowship.

REFERENCES

- [1] The Department of Energy, "The Future of Geothermal Energy," 2006. Available online: <http://energy.gov/eere/geothermal/future-geothermal-energy>
- [2] H. Xiao, J. Deng, Z. Wang, and W. Huo, "Fiber optic pressure sensor with self-compensation capability for harsh environment applications," *Optical Engineering*, vol. 44, issue 5, 2005.
- [3] L. Chen and M. Mehregany, "A silicon carbide capacitive pressure sensor for in-cylinder pressure measurement," *Sensors Actuators A Phys.*, vol. 145–146, pp. 2–8, Jul. 2008.
- [4] S. . Moe, K. Schjølberg-Henriksen, D. . Wang, E. Lund, J. Nysæther, L. Furuberg, M. Visser, T. Fallet, and R. . Bernstein, "Capacitive differential pressure sensor for harsh environments," *Sensors Actuators A Phys.*, vol. 83, no. 1, pp. 30–33, 2000.
- [5] A. C. McNeil and Y. Lin, "Pressure sensor with differential capacitive output," US 20140060169 A1, 2012.
- [6] D. R. Harrison and J. Dimeff, "A Diode-Quad Bridge Circuit for Use with Capacitance Transducers," *Rev. Sci. Instrum.*, vol. 44, no. 10, p. 1468, 1973.
- [7] W. P. Eaton and J. H. Smith, "Micromachined pressure sensors: review and recent developments," *Smart Mater. Struct.*, vol. 6, no. 5, pp. 530–539, Oct. 1997.
- [8] R. J. Roark, W. C. Young, and R. G. Budynas, *Roark's formulas for stress and strain*. McGraw-Hill, 2002.